

# Accretion and outflow of gas in Markarian 509

Jelle Kaastra<sup>1,2</sup>, Pierre-Olivier Petrucci<sup>3</sup>, Massimo Cappi<sup>4</sup>,  
Nahum Arav<sup>5</sup>, Ehud Behar<sup>6</sup>, Stefano Bianchi<sup>7</sup>, Graziella  
Branduardi-Raymont<sup>8</sup>, Elisa Costantini<sup>1</sup>, Jacobo Ebrero<sup>1</sup>,  
Jerry Kriss<sup>9,10</sup>, Missagh Mehdipour<sup>8</sup>, Stephane Paltani<sup>11</sup>, Ciro Pinto<sup>1</sup>,  
Gabriele Ponti<sup>12</sup>, Katrien Steenbrugge<sup>13,14</sup> and Cor de Vries<sup>1</sup>

<sup>1</sup>SRON Netherlands Institute for Space Research, Sorbonnelaan 2,  
3584 CA Utrecht, The Netherlands  
email: j.kaastra@sron.nl

<sup>2</sup>Utrecht University, Utrecht, The Netherlands

<sup>3</sup>UJF-Grenoble 1 / CNRS-INSU, Institut de Planétologie et d'Astrophysique de Grenoble  
(IPAG) UMR 5274, Grenoble 38041, France

<sup>4</sup>INAF-IASF Bologna, via Gobetti 101, 40129 Bologna, Italy

<sup>5</sup>Department of Physics, Virginia Tech, Blacksburg, VA 24061, USA

<sup>6</sup>Department of Physics, Technion-Israel Institute of Technology, 32000 Haifa, Israel

<sup>7</sup>Dipartimento di Fisica, Università degli Studi Roma Tre, via della Vasca Navale 84,  
00146 Roma, Italy

<sup>8</sup>Mullard Space Science Laboratory, University College London, Holmbury St. Mary, Dorking,  
Surrey, RH5 6NT, UK

<sup>9</sup>Space Telescope Science Institute, 3700 San Martin Drive, Baltimore, MD 21218, USA

<sup>10</sup>Department of Physics and Astronomy, The Johns Hopkins University, Baltimore,  
MD 21218, USA

<sup>11</sup>ISDC Data Centre for Astrophysics, Astronomical Observatory of the University of Geneva,  
16, ch. d'Ecogia, 1290 Versoix, Switzerland

<sup>12</sup>Max-Planck Institut für Extraterrestrische Physik, Garching, Germany

<sup>13</sup>Instituto de Astronomía, Universidad Católica del Norte, Avenida Angamos 0610, Casilla  
1280, Antofagasta, Chile

<sup>14</sup>Department of Physics, University of Oxford, Keble Road, Oxford OX1 3RH, UK

**Abstract.** A major uncertainty in models for photoionised outflows in AGN is the distance of the gas to the central black hole. We present the results of a massive multiwavelength monitoring campaign on the bright Seyfert 1 galaxy Mrk 509 to constrain the location of the outflow components dominating the soft X-ray band. Mrk 509 was monitored by XMM-Newton, Integral, Chandra, HST/COS and Swift in 2009. We have studied the response of the photoionised gas to the changes in the ionising flux produced by the central regions. We were able to put tight constraints on the variability of the absorbers from day to year time scales. This allowed us to develop a model for the time-dependent photoionisation in this source. We find that the more highly ionised gas producing most X-ray line opacity is at least 5 pc away from the core; upper limits to the distance of various absorbing components range between 20 pc up to a few kpc. The more lowly ionised gas producing most UV line opacity is at least 100 pc away from the nucleus. These results point to an origin of the dominant, slow ( $v < 1000 \text{ km s}^{-1}$ ) outflow components in the NLR or torus-region of Mrk 509. We find that while the kinetic luminosity of the outflow is small, the mass carried away is likely larger than the 0.5 Solar mass per year accreting onto the black hole. We also determined the chemical composition of the outflow as well as valuable constraints on the different emission regions. We find for instance that the resolved component of the Fe-K line originates from a region 40–1000 gravitational radii from the black hole, and that

the soft excess is produced by Comptonisation in a warm (0.2–1 keV), optically thick ( $\tau \sim 10$ –20) corona near the inner part of the disk.

**Keywords.** Active Galactic Nuclei, X-rays, outflows

## 1. Introduction

Active Galactic Nuclei (AGN) are powered by accretion onto a super-massive black hole. In addition to the accretion process, however, it has been found that many AGN contain strong outflows. The total mass loss associated with this outflow may even be larger than the mass that finally reaches the black hole, and the kinetic energy associated with the outflow may be large enough to regulate the growth of the black hole and tightly connected to it, the growth of the host galaxy.

Different origins for these outflows or winds have been proposed, like accretion disk winds, thermal evaporation from the torus, or extended ionisation cones. These models all imply very different effects for the impact of the outflow on the environment, the feedback process. First, outflows launched close to the black hole (like accretion disk winds) have to overcome a larger gravitational potential to escape, hence should have much larger outflow velocities  $v$ , from thousands of  $\text{km s}^{-1}$  to significant fractions of the speed of light. Furthermore, outflows at larger distances  $r$  from the black hole (like e.g. torus winds) have a larger impact on the surroundings, because we have for the mass loss rate  $\dot{M}$ :

$$\dot{M}/\Omega = N_{\text{H}} m_p r v, \quad (1.1)$$

with  $\Omega$  the solid angle subtended by the outflow,  $m_p$  the proton mass and  $N_{\text{H}}$  the total column density. The kinetic luminosity  $L_K$  is simply given by  $\frac{1}{2}\dot{M}v^2$ .

While column densities and outflow velocities can be obtained directly from the spectrum, the distance should be obtained by other means. Given the ionisation parameter  $\xi = L/nr^2$  with  $L$  the ionising luminosity and  $n$  the hydrogen density, a known value for  $n$  immediately gives  $r$ , because  $L$  and  $\xi$  are known from observations. Because the recombination time scale of the plasma scales with  $n^{-1}$ , the delay time of the ionisation state of the plasma with respect to variations of the continuum luminosity immediately yields the density and therefore the distance of the absorber. This is the principle that forms the basis for our large monitoring campaign on Mrk 509, a bright and luminous Seyfert 1 galaxy at  $z = 0.034$ .

## 2. The monitoring campaign on Mrk 509

We have observed Mrk 509 intensively during a 100-day campaign in 2009 (Kaastra *et al.* 2011a). The core of the campaign consisted of  $10 \times 60$  ks observations with XMM-Newton, spaced 4 days, coincident with ten INTEGRAL observations of 120 ks each. This was followed by a 180 ks observation with the Chandra LETGS, simultaneous with 10 orbits HST/COS. It was preceded with Swift monitoring (UV, X-ray) and supplemented with ground-based observations (WHT, Pairitel). Up to now, 12 refereed papers have been published on this campaign and more are under preparation.

The lightcurve of Mrk 509 (Kaastra *et al.* 2011a) showed the expected variability with a large ( $\sim 60\%$  increase) outburst in the middle of our campaign. Our first step was to determine the time-averaged spectrum. Because of the high statistical quality of the data, special analysis tools and refinements to the calibration needed to be developed, in particular for the RGS instruments of XMM-Newton (Kaastra *et al.* 2011b), but also for

the EPIC camera (Ponti *et al.* 2012) and the Optical Monitor (Mehdipour *et al.* 2011) of XMM-Newton and the HST/COS spectrometer (Kriss *et al.* 2011).

The time-averaged spectrum showed five different ionisation components producing significant absorption lines in the RGS spectrum (Detmers *et al.* 2011). These results were confirmed by the LETGS spectra (Ebrero *et al.* 2011). The quality of the data was high enough to prove for the first time that two of the ionisation components, C and D, are discrete structures with a FWHM of less than 35 and 80%, respectively. However, these components are *not* in pressure equilibrium. From component A to E, the gas pressure drops by two orders of magnitude. For a proper modeling of the ionisation structure the spectral energy distribution (SED) of the source needs to be known accurately, and thanks to our broad-band coverage from optical to hard X-ray wavelengths we were able to do this modeling.

The next step was to constrain the distance  $r$  of the absorbers, by measuring the delayed response of the absorbers with respect to the continuum variations. To do this properly, we developed a time-dependent photo-ionisation model. Starting with equilibrium, we followed the spectral variations over time and calculated the ion concentrations for different gas densities  $n$ . Comparing the predicted changes in absorber transmission for each of these models with the observed spectra, the distances could be constrained (Kaastra *et al.* 2012). For components C–E no significant variability during our campaign was found, leading to lower limits of their distance. However, component D showed evidence for variability on long time scales, by comparison with archival spectra taken in 2000 and 2001, yielding a tight upper limit to its distance. For components C and E upper limits were derived from the requirement that  $r < L/N_{\text{H}}\xi$ . Our measurements were not sensitive enough to constrain variability for components A and B, but O III is present in component A, and through direct imaging of its forbidden 5007 Å line its distance has been determined to be  $\sim 3$  kpc (Phillips *et al.* 1983). Furthermore, from variability constraints of the UV line velocity components, corresponding to ionisation components A and B, Arav *et al.* (2012) derived lower limits of  $\sim 200$  pc for most of them.

Fig. 1 summarises the distance limits. The dominant X-ray absorption components C–E originate from a region outside the inner torus radius. Thus, these outflow components are more likely explained by torus winds rather than accretion disk winds.

Using several arguments, the total mass loss of the wind is between 0.26 and 2100 solar masses per year. This is large compared to the accretion rate of about 0.5 solar mass per year. However, due to the limited outflow velocities of the wind (up to several  $100 \text{ km s}^{-1}$ , but not relativistic), the kinetic luminosity of the outflow is not very large.

Our spectra also yielded the metal abundances of the outflow. Steenbrugge *et al.* (2011) measured the abundances of C, N, Ne, Mg, Si, S, Ca and Fe relative to iron with accuracies down to 8% for some elements. The ratios agree fairly well with solar abundances, although we could not yet constrain the absolute abundances. We will determine those later using new HST/COS spectra covering better the Lyman series of hydrogen.

The Galactic foreground absorption was studied by Pinto *et al.* (2012). The UV spectrum shows seven discrete absorption structures. Some of these are associated to high-velocity clouds, others correspond to absorption within the spiral arms of our Galaxy. A detailed assessment of the role of dust and gas at various temperatures could be made.

The UV lightcurve shows a distinct outburst near the centre of our monitoring campaign. The soft X-ray flux correlates very well with these variations in the UV flux, while the hard X-ray flux does not correlate at all with the other bands. This and the spectral shape led Mehdipour *et al.* (2011) to conclude that the soft X-ray excess in Mrk 509 is not caused by blurred reflection, but by comptonisation of the soft UV photons of the

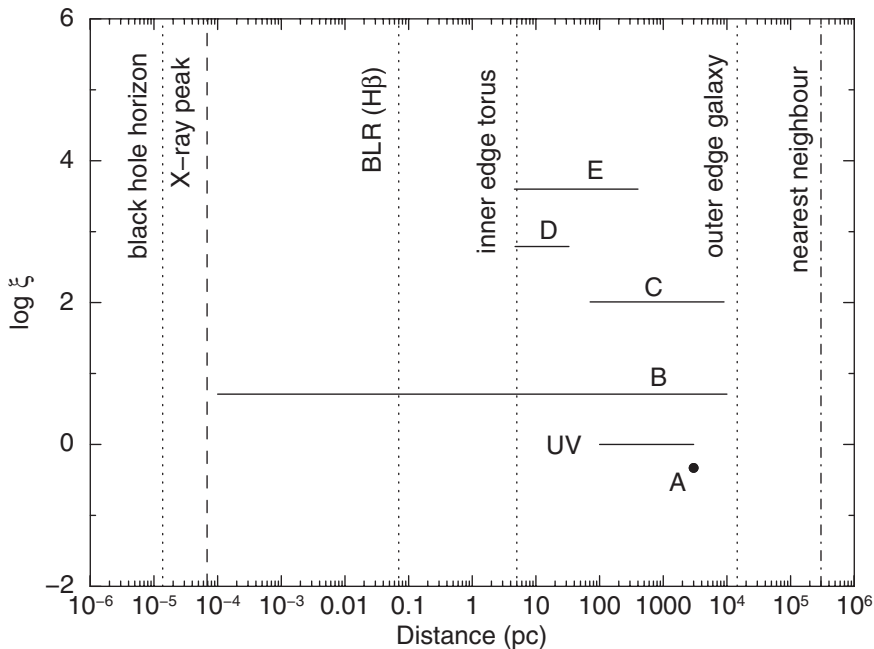


**Figure 1.** Distances of the absorption components in Mrk 509. Horizontal bars indicate the allowed ranges for each of the individual absorption components. The x-axis gives distances from the black hole, the y-axis the ionisation parameter  $\xi$  for each component A–E. The constraint from the UV lines, a mixture of ionisation components A and B, is also shown. Vertically dashed lines indicate some radii of interest.

disk. Further detailed modeling by Petrucci *et al.* (2012) strengthened this picture. The scattering medium has a large optical depth of  $\sim 15$ , at a temperature of  $\sim 1$  keV.

Finally, Ponti *et al.* (2012) studied the Fe-K emission line, showing that the neutral component consists of a narrow, constant component, possibly originating from material between the outer broad-line region and the torus, and a broad variable component, originating from the inner broad line region.

## References

- Arav, N., Edmonds, D., Borguet, B., *et al.* 2012, *A&A*, 544, A33  
 Detmers, R. G., Kaastra, J. S., Steenbrugge, K. C., *et al.* 2011, *A&A*, 534, A38  
 Ebrero, J., Kriss, G. A., Kaastra, J. S., *et al.* 2011, *A&A*, 534, A40  
 Kaastra, J. S., Petrucci, P.-O., Cappi, M., *et al.* 2011a, *A&A*, 534, A36  
 Kaastra, J. S., de Vries, C. P., Steenbrugge, K. C., *et al.* 2011b, *A&A*, 534, A37  
 Kaastra, J. S., Detmers, R. G., Mehdipour, M., *et al.* 2012, *A&A*, 539, A117  
 Kriss, G. A., Arav, N., Kaastra, J. S., *et al.* 2011, *A&A*, 534, A41  
 Mehdipour, M., Branduardi-Raymont, G., Kaastra, J. S., *et al.* 2011, *A&A*, 534, A39  
 Petrucci, P.-O., Paltani, S., Malzac, J., *et al.* 2012, *A&A*, in press (arXiv1209.6438)  
 Phillips, M. M., Bladwin, J. A., Atwood, B., & Carswell, R. F. 1983, *ApJ*, 274, 558  
 Pinto, C., Kriss, G. A., Kaastra, J. S., *et al.* 2012, *A&A*, 541, A147  
 Ponti, G., Cappi, M., Costantini, E., *et al.* 2012, *A&A*, in press (arXiv1207.0831)  
 Steenbrugge, K. C., Kaastra, J. S., Detmers, R. G., *et al.* 2011, *A&A*, 534, A42